Heredity (2010) 104, 302–309

www.nature.com/hdy

ORIGINAL ARTICLE

A comparison of recombination frequencies in intraspecific versus interspecific mapping populations of *Nasonia*

LW Beukeboom[1], O Niehuis[2,3], BA Pannebakker[1,4], T Koevoets[1], JD Gibson[2], DM Shuker[4,5], L van de Zande[1] and J Gadau[2]

[1]*Evolutionary Genetics, Centre for Ecological and Evolutionary Studies, University of Groningen, Haren, The Netherlands;* [2]*School of Life Sciences, Arizona State University, Tempe, AZ, USA;* [3]*Behavioural Biology, University of Osnabrück, Osnabrück, Germany and* [4]*Institute of Evolutionary Biology, School of Biological Sciences, University of Edinburgh, Edinburgh, UK*

We present the first intraspecific linkage map for *Nasonia vitripennis* based on molecular markers. The map consists of 36 new microsatellite markers, extracted from the *Nasonia* genome sequence, and spans 515 cM. The five inferred linkage groups correspond to the five chromosomes of *Nasonia*. Comparison of recombination frequencies of the marker intervals spread over the whole genome ($N = 33$ marker intervals) between the intraspecific *N. vitripennis* map and an interspecific *N. vitripennis* × *N. giraulti* map revealed a slightly higher (1.8%) recombination frequency in the intraspecific cross. We further considered an *N. vitripennis* × *N. longicornis* map with 29 microsatellite markers spanning 430 cM. Recombination frequencies in the two interspecific crosses differed neither between reciprocal crosses nor between mapping populations of embryos and adults. No major chromosomal rearrangements were found for the analyzed genomic segments. The observed differential F_2 hybrid male mortality has no significant effect on the genome-wide recombination frequency in *Nasonia*. We conclude that interspecific crosses between the different *Nasonia* species, a hallmark of *Nasonia* genetics, are generally suitable for mapping quantitative and qualitative trait loci for species differences.
Heredity (2010) **104,** 302–309; doi:10.1038/hdy.2009.185; published online 20 January 2010

Keywords: hybrids; linkage map; microsatellites; recombination; insects; speciation

Introduction

Genetic linkage maps are essential for the genetic analysis of biological traits. For example, research on the identification of the genetic architecture of quantitative traits relies heavily on the availability of linkage maps. Owing to the recent developments in DNA marker technologies, linkage maps are now available for many plant and animal species. Although this is true for many non-model as well as model organisms, the availability of the whole genome sequence for a model organism still greatly facilitates the rapid development of large numbers of reliable markers and, as a consequence, detailed linkage mapping using high throughput techniques. Traditionally, RAPD and AFLP markers were used in the absence of genome sequences because RAPD and AFLP genotyping was the only way to analyze a large number of variable markers necessary for linkage mapping. However, these markers are inherently difficult to interpret and are plagued with low reproducibility. The most commonly applied alternatives, microsatellites and single nucleotide polymorphism markers are more informative and robust, but their development typically requires a relatively large investment in terms of time and resources. The availability of genome sequence information avoids the costly cloning and sequencing efforts needed to detect markers, and one can detect markers and develop oligonucleotide primers for polymerase chain reaction (PCR) *in silico*. This approach allows for the rapid development of hundreds of microsatellite and single nucleotide polymorphism markers. An additional advantage of having the physical genome sequence of a study organism available is that one can use positional information to select markers with equal recombinational spacing across the genome (for example a marker every 20 cM), which greatly facilitates mapping of traits of interest. Moreover, one can compare local recombination frequencies with features of the physical map position to identify, for example, recombination hotspots, chromosomal inversions, and gene-rich genomic segments (Petes, 2001; Myers *et al*., 2005; Kulathinal *et al*., 2008; Niehuis *et al*., 2010; Werren *et al*., 2010).

Genetic linkage maps are now available for many insect species (Wilfert *et al*., 2007; Hunter and Kole, 2008). However, high-density maps are still restricted to species whose genomes have been sequenced: fruit flies of the genus *Drosophila* (Chen *et al*., 2009), the yellow fever mosquito *Aedes aegypti* (Fulton *et al*., 2001), the red flour beetle *Tribolium castaneum* (Lorenzen *et al*., 2005), the

Correspondence: Dr LW Beukeboom, Centre for Ecological and Evolutionary Studies, University of Groningen, PO Box 14, Haren NL-9750 AA, The Netherlands.
E-mail: l.w.beukeboom@rug.nl
[5]*Current address: School of Biology, University of St Andrews, St Andrews, KY16 9TH, UK*
Received 7 May 2009; revised 16 October 2009; accepted 10 December 2009; published online 20 January 2010

silkworm *Bombyx mori* (Yamamoto *et al*., 2006), and the honey bee *Apis mellifera* (Solignac *et al*., 2007). Here, we are concerned with the parasitoid (jewel) wasp *Nasonia vitripennis*, whose complete genome sequence has recently been published together with that of its closely related congeners *N. giraulti* and *N. longicornis* (Werren *et al*., 2010).

N. vitripennis has been used for genetic studies for over 60 years. Its suitability as an experimental organism stems largely from its ease of culturing in the laboratory and its haplodiploid mode of sex determination (*Nasonia* males are haploid). Saul (1993) published the first comprehensive linkage map for *N. vitripennis*, summarizing information of earlier mapping studies by, among others, Saul and Kayhart (1956) and Whiting (1967). This classical *Nasonia* map consists of 47 visible mutant markers in five linkage groups, consistent with the haploid complement of $N=5$ chromosomes. In recent years, *Nasonia* has become an important model organism in evolutionary, ecological, and developmental genetics, which culminated in the *Nasonia* genome project (Werren *et al*., 2010). The intense interest in this organism, in combination with the development of DNA marker technologies, has resulted in several efforts to construct molecular marker linkage maps for *Nasonia* (Gadau *et al*., 2008). The first linkage map using molecular markers for *Nasonia* stems from the pre-genome sequence era and was inferred using RAPD markers (Gadau *et al*., 1999). The first microsatellite loci of *Nasonia* were published by Pietsch *et al*. (2004), and, in the same year, Rütten *et al*. (2004) developed chromosome-specific microsatellite markers from microcloned chromosomes. This made it possible to homologize the earlier inferred linkage groups of *Nasonia* (Saul, 1993; Gadau *et al*., 1999) with its five chromosomes (Gokhman and Westendorf, 2000). Niehuis *et al*. (2008) then published an interspecific *N. vitripennis* × *N. giraulti* map containing 38 molecular markers. The most recent linkage map for *Nasonia* is based on a large number of interspecific single nucleotide polymorphism markers identified from the annotated *Nasonia* genome sequences (1255 markers; Niehuis *et al*., 2010).

The genus *Nasonia* currently includes four species: *N. vitripennis*, *N. longicornis*, *N. giraulti*, and *N. oneida*; the latter being described in this issue (Raychoudhury *et al*., 2010). The divergence of *N. vitripennis* and the other three species is estimated to be around 1 mya, and that of *N. longicornis* and *N. giraulti* about 0.2 mya (Campbell *et al*., 1993). The *Nasonia* species complex has become especially instructive for genetic analysis of species differences, because all the species can be crossed and genomic segments easily exchanged between species. As such, a number of studies have used linkage maps constructed from interspecific crosses. However, an intraspecific *Nasonia* map based on molecular markers has yet to be published. Importantly, linkage maps based on interspecific crosses may yield incorrect recombination distance estimates between markers or genes of interest because of hybridization artifacts. Specifically, recombination frequencies may be increased or decreased when combining genomes of two species because of major genome reorganizations or the release of recombination suppressors (Trickett and Butlin, 1994; Zhang *et al*., 1999). Moreover, the recovery of alleles may be affected by nuclear–nuclear and nuclear–cytoplasmic genic incompatibilities, both of which are known to occur in *Nasonia* hybrids (Breeuwer and Werren, 1995; Gadau *et al*., 1999; Niehuis *et al*., 2008). Weston *et al*. (1999) have presented a formal model, which suggested that hybrid mortality because of nucleo–nucleo genic incompatibilities can lead to pseudo-linkage and thus the inference of a false marker order. To test for marker transmission ratio distortion (MTRD) in *Nasonia* hybrids, Niehuis *et al*. (2008) compared marker allele frequencies between embryos and adults. They found that some markers indeed show a significantly distorted recovery in adults compared with embryos and attributed the MTRD to mortality associated with particular genotypes during larval development. However, to what extent MTRD in hybrids impacts on the accuracy of interspecific linkage maps remains to be tested.

Here, we present the first intraspecific linkage map for *N. vitripennis* based on molecular markers. Considering the chromosome-anchored markers developed by Rütten *et al*. (2004), we were able to associate the original linkage groups of *N. vitripennis* distinguished by Saul (1993) with the five *Nasonia* chromosomes. We contrast recombination frequencies of homologous genomic segments between the intraspecific *N. vitripennis* cross and an interspecific *N. vitripennis* × *N. giraulti* mapping population of embryos that showed no MTRD using the data published by Niehuis *et al*. (2010). We next compare recombination frequencies of embryos with those of adults in two interspecific crosses (that is *N. vitripennis* × *N. longicornis* and *N. vitripennis* × *N. giraulti*) to determine the effect of MTRD on recombination estimates and marker order. Finally, we test for differences in recombination frequencies between both reciprocal crosses of the two interspecific mapping populations to screen for non-recombining genome segments.

Materials and methods

Microsatellite marker selection

We used the position and properties of microsatellite markers from an *in silico* screen of the *N. vitripennis* genome sequences (Werren *et al*., 2010) conducted by Pannebakker *et al*. (2010). We selected microsatellite markers primarily on the largest *N. vitripennis* scaffolds and looked for flanking sequences with ortholog sequences in the *N. giraulti* and *N. longicornis* trace sequence archives. We initially selected two microsatellite markers per scaffold, one on either end, to be able to map and orient the scaffolds along the chromosomes. Although the microsatellite markers of the Nv100 series (see Supplementary Table 1) were specifically screened for polymorphisms within *N. vitripennis*, those of the Nv300 series were tailored to match and/or replace molecular markers that had been used by Niehuis *et al*. (2008) to infer an *N. giraulti* × *N. vitripennis* framework map.

Mapping populations and marker genotyping

All earlier mapping efforts in *Nasonia* exploited the advantage of haploid males. Typically, two parental lines differing in allele composition were crossed. The resulting F_1 females layed eggs as virgins, yielding recombinant F_2 males that carry either one of the grandparental alleles.

Intraspecific *N. vitripennis* map: An initial screen of a number of different field strains for genetic variation (Pannebakker *et al*., 2008) provided two strains that showed allelic differences in a large number of loci: C222a (collected in 2003 by LW Beukeboom) and HV6 (collected in 2004 by T Koevoets, MN Burton-Chellew, and EM Sykes; for collection details see Burton-Chellew *et al*. (2008)). Both strains originated from De Hoge Veluwe in the Netherlands and were set up and maintained as iso-female lines (that is started as a line from a single mated female). A total of 276 F_2 adult males of a cross between a C222a male and a HV6 female were genotyped for 41 microsatellite markers that are polymorphic between these two strains (36 of these markers could be mapped). DNA was extracted using 5% Chelex 100 solution (Bio-Rad, Hercules, CA, USA). PCR amplifications of microsatellite markers of the Nv100 series were performed in 10.0 µl volumes ($1 \times NH_4$ buffer, 10 mM $MgCl_2$, 1 mM dNTP mix, 4 mM of each primer, 0.5 units BIOTAQ DNA polymerase (Bioline Ltd., London, UK), 2 µl DNA (20 ng)). The PCR temperature profile started with a 4 min denaturation step at 94 °C followed by 39 cycles of 30 s at 94 °C, 30 s at the annealing temperature (T_a) specified in Supplementary Table 1, and 1 min at 72 °C, followed by 10 min at 72 °C. Differences in the length of the PCR products were determined on 4% Tris–acetate–EDTA agarose gels stained with ethidium bromide. Gels were run on a Sub-Cell Model 96 electrophoresis cell (Bio-Rad) at 120 V for a length of ~5 cm.

Interspecific *N. vitripennis* × *N. girault*i map: We analyzed genotype data of 120 embryonic and of 120 adult F_2 hybrid males of reciprocal crosses between *N. vitripennis* (AsymCX) and *N. girault*i (RV2X) (see Niehuis *et al*., 2008, for methodological details). This allowed for a comparison of the recombination frequencies between embryos and adults within crosses and of embryos and adults between reciprocal crosses. All individuals had been genotyped for 38 single nucleotide polymorphism markers by Niehuis *et al*. (2008).

Interspecific *N. vitripennis* × *N. longicornis* map: In a similar manner to the *N. vitripennis* × *N. girault*i interspecific cross, we genotyped 120 embryonic and 120 adult F_2 hybrid males of each reciprocal cross between *N. vitripennis* (AsymCX) and *N. longicornis* (IV7(U)). However, this time we used microsatellite markers that had been developed to match the molecular markers used by Niehuis *et al*. (2008). PCR amplification of the microsatellite markers of the Nv300 was conducted with the Qiagen multiplex PCR kit for five different sets according to the manufacturer's recommendations and applying Applied Biosystems Veriti and Applied Biosystems 9700 thermocyclers. The PCR temperature profile started with a 15 min denaturation step at 95 °C followed by 30 cycles of 30 s at 94 °C, 1 min 30 s at the annealing temperature (T_a) specified in Supplementary Table 1, and 1 min at 72 °C, followed by 45 min at 72 °C. All amplicons of the Nv300 microsatellite marker series were separated on an Applied Biosystems 3730 DNA Analyzer and analyzed with the software GeneMapper v4.0 (Applied Biosystems, Foster City, CA, USA).

Marker segregation data were analyzed with the software Multipoint (http://multiqtl.com), which infers marker order and map distances using a multipoint likelihood approach (Mester *et al*., 2003a,b, 2004). We calculated pairwise recombination fractions for all pairs of markers using the Kosambi mapping function (Kosambi, 1944).

Comparison of recombination frequencies

We compared recombination frequencies only between adjacent markers that were shared by the two respective populations. If a marker was present in only one of the two compared mapping populations, we excluded it from the analysis. In some cases, markers could not be unambiguously placed on the map. However, it was still possible to use them to estimate pairwise recombination frequencies (see Table 1). In some instances, the two maps differed in marker order, in which case the STS map of Niehuis *et al*. (2010) was used as template.

Intraspecific *N. vitripennis* versus interspecific *N. vitripennis* × *N. girault*i F_2 hybrid embryos: To match the microsatellite markers used in the *N. vitripennis* intraspecific cross with the molecular markers that had been analyzed in the interspecific *N. girault*i (♂) × *N. vitripennis* (♀) cross, we searched for molecular markers in the interspecific map that were physically closest to the newly developed microsatellite markers (Nv100 series). Of the 38 microsatellite loci on the intraspecific map that we matched to the molecular markers on the interspecific map (Niehuis *et al*., 2008), one was identical (Nv319) and the remaining 37 showed an average distance of 0.2% recombination (range 0–2.7% recombination, see Supplementary Table 2) based on the high-density linkage map published by Niehuis *et al*. (2010).

Embryo versus adult F_2 hybrids: As a subset of markers were similarly genotyped in embryo and adult *N. vitripennis* × *N. girault*i F_2 hybrid males, as well as in *N. vitripennis* × *N. longicornis* F_2 hybrid males, we were able to compare recombination frequencies between marker pairs directly.

Interspecific *N. vitripennis* × *N. girault*i versus interspecific *N. vitripennis* × *N. longicornis* F_2 hybrids: To compare recombination frequencies between the *N. vitripennis* × *N. girault*i and *N. vitripennis* × *N. longicornis* interspecific crosses, molecular markers studied by Niehuis *et al*. (2008) were again matched for location with existing microsatellite markers (mostly Nv300 series). Of those matches, one was identical (Nv26) and 16 were on average separated by 1.0% recombination (range 0–5.4% recombination, see Supplementary Table 3).

Results

Linkage maps

In total, we developed 53 new dinucleotide and 3 trinucleotide microsatellite markers (together comprising the Nv100 and Nv300 marker series) from the *Nasonia* genome assembly 1.0 (Supplementary Table 1). For many of those loci, the three *Nasonia* strains sequenced in the *Nasonia* genome sequencing project had fixed allelic differences, and 35 of these new markers (plus one old

Table 1 Markers and recombination frequency estimates used in the comparison between the intraspecific mapping population of adult male *N. vitripennis* and the interspecific mapping population of *N. girault*i (♂) × *N. vitripennis* (♀) F_2 hybrid embryos (see Figure 2)

Chromosome	*Adjacent microsatellite marker pair of intraspecific N. vitripennis map*	*Recombination rate estimate in N. vitripennis adults (cM)*	*Corresponding adjacent scaffold positions in N. vitripennis genome*	*Recombination rate estimate in N. vitripennis-N. girault*i *embryos (cM)*
1	Nv180-Nv181	0.145	NVG_SCAFFOLD16_1815958-NVG_SCAFFOLD16_3425262	0.143
1	Nv181-Nv126[a]	0.197	NVG_SCAFFOLD16_3425262-NVG_SCAFFOLD41_300676	0.181
1	Nv126-Nv156[a]	0.000	NVG_SCAFFOLD41_300676-NVG_SCAFFOLD73_410408	0.000
1	Nv156-Nv170[a]	0.000	NVG_SCAFFOLD73_410408-NVG_SCAFFOLD170_1506160	0.008
1	Nv170-Nv191[a]	0.045	NVG_SCAFFOLD170_1506160-NVG_SCAFFOLD33_767863	0.000
1	Nv191-Nv169[a]	0.000	NVG_SCAFFOLD33_767863-NVG_SCAFFOLD25_803967	0.000
1	Nv169-Nv105[a]	0.136	NVG_SCAFFOLD25_803967-NVG_SCAFFOLD1_2289896	0.039
1	Nv105-Nv127[a]	0.221	NVG_SCAFFOLD1_2289896-NVG_SCAFFOLD60_741110	0.136
2	Nv193-Nv20	0.352	NVG_SCAFFOLD8_907155-NVG_SCAFFOLD31_231950	0.274
2	Nv20-Nv168[b]	0.063	NVG_SCAFFOLD31_231950-NVG_SCAFFOLD15_2695394	0.159
2	Nv168-Nv123	0.027	NVG_SCAFFOLD15_2695394-NVG_SCAFFOLD13_2593414	0.023
2	Nv123-Nv132	0.012	NVG_SCAFFOLD13_2593414-NVG_SCAFFOLD19_473227	0.012
2	Nv132-Nv133	0.071	NVG_SCAFFOLD19_473227-NVG_SCAFFOLD19_2929250	0.063
2	Nv133-Nv186	0.211	NVG_SCAFFOLD19_2929250-NVG_SCAFFOLD24_1685756	0.199
2	Nv186-Nv190	0.214	NVG_SCAFFOLD24_1685756-NVG_SCAFFOLD309_48837	0.213
3	Nv319-Nv192	0.264	NVG_SCAFFOLD18_2635495-NVG_SCAFFOLD6_1855275	0.271
3	Nv192-Nv189	0.054	NVG_SCAFFOLD6_1855275-NVG_SCAFFOLD44_4553601	0.071
3	Nv189-Nv184	0.072	NVG_SCAFFOLD44_4553601-NVG_SCAFFOLD22_1311250	0.056
3	Nv184-Nv111	0.151	NVG_SCAFFOLD22_1311250-NVG_SCAFFOLD17_1342149	0.099
3	Nv111-Nv108	0.175	NVG_SCAFFOLD17_1342149-NVG_SCAFFOLD28_187258	0.177
3	Nv108-Nv107	0.139	NVG_SCAFFOLD28_187258-NVG_SCAFFOLD28_1356359	0.141
4	Nv26-Nv141	0.378	NVG_SCAFFOLD4_2791862-NVG_SCAFFOLD29_1439582	0.285
4	Nv141-Nv114[b]	0.027	NVG_SCAFFOLD29_1439582-NVG_SCAFFOLD23_1489254	0.054
4	Nv114-Nv147[b]	0.027	NVG_SCAFFOLD23_1489254-NVG_SCAFFOLD34_1272544	0.008
4	Nv147-Nv136[a]	0.018	NVG_SCAFFOLD34_1272544-NVG_SCAFFOLD26_7306	0.011
4	Nv136-Nv137[a]	0.004	NVG_SCAFFOLD26_7306-NVG_SCAFFOLD26_1516282	0.004
4	Nv137-Nv182	0.090	NVG_SCAFFOLD26_1516282-NVG_SCAFFOLD123_174844	0.065
4	Nv182-Nv154	0.202	NVG_SCAFFOLD123_174844-NVG_SCAFFOLD9_3107879	0.162
4	Nv154-Nv104	0.329	NVG_SCAFFOLD9_3107879-NVG_SCAFFOLD9_635808	0.318
5	Nv124-Nv179	0.291	NVG_SCAFFOLD14_227534-NVG_SCAFFOLD14_3478710	0.287
5	Nv179-Nv152	0.105	NVG_SCAFFOLD14_3478710-NVG_SCAFFOLD38_42794	0.038
5	Nv152-Nv176	0.185	NVG_SCAFFOLD38_42794-NVG_SCAFFOLD1_6038985	0.127
5	Nv176-Nv109	0.008	NVG_SCAFFOLD1_6038985-NVG_SCAFFOLD1_7302524	0.007

The recombination rate estimates are based on the number of recombinant individuals for each pair of adjacent markers shared in both crosses. Deviations in marker composition and position from the map in Figure 1 are due to the non-mapping of certain markers.
[a]Incongruent marker sequence: the scaffold positions are taken as template.
[b]Not in intraspecific *N. vitripennis* map.

marker, Nv26) could be mapped using the intraspecific *N. vitripennis* mapping population.

Intraspecific *N. vitripennis* map: The map is based on a cross between two *N. vitripennis* field strains (C222a and HV6) and has a size of 515 cM. The studied microsatellite markers are distributed over all five linkage groups, representing the five chromosomes. The average marker spacing is 10.0 cM (Figure 1).

Interspecific *N. vitripennis* × *N. longicornis* map: The microsatellite markers used to infer the map were closely linked to the molecular markers studied by Niehuis *et al*. (2008). The map consists of 29 microsatellite markers in five linkage groups and spans 438 cM (the map will be published elsewhere).

Comparison of recombination frequencies

Intraspecific versus interspecific recombination frequencies: We compared the recombination frequencies of 33 genome segments distributed over the entire linkage map for adult *N. vitripennis* males (map size 515 cM, average segment size 12.8 cM) and interspecific *N. vitripennis* × *N. girault*i embryos with *girault*i cytoplasm (map size 381.5 cM, average segment size 11.0 cM; Niehuis *et al*., 2008; see Table 1). The 33 marker intervals span a total of 313.5 cM, which is about 70% of the saturated high-density genome map (Niehuis *et al*., 2010). We chose to use embryos of the interspecific cross to eliminate the possible effect of hybrid incompatibilities on recombination, potentially allowing us to identify genome reorganizations. Embryos of this particular cross do not show significant MTRD (Niehuis *et al*., 2008). Pairwise comparison of recombination frequencies between the intraspecific and the interspecific map revealed a slightly higher (1.8%) intraspecific recombination rate on a genome-wide level ($N = 33$ genomic segments, Wilcoxon matched-pairs test, $P = 0.005$; Figure 2). Chromosome 1 and 5 show the largest deviations. This partly results from

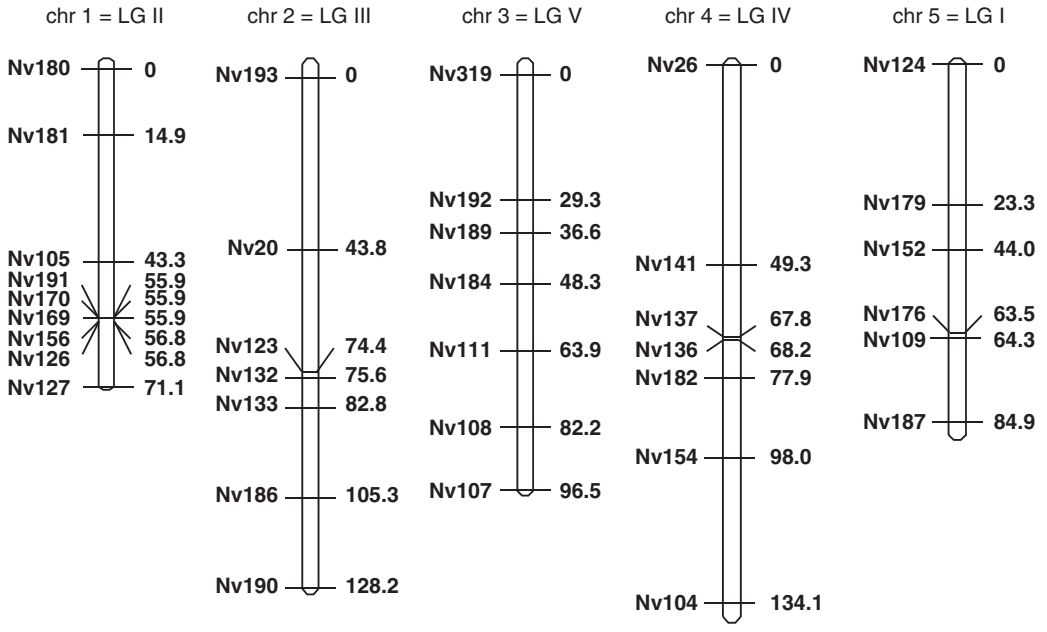

Figure 1 Genetic linkage map for *N. vitripennis*. The map comprises 36 microsatellite markers on five linkage groups, spanning a total of 515 cM. Saul's (1993) linkage groups were linked with the chromosome numbers by Rütten *et al*. (2004). Markers are shown on the left-hand side of each chromosome and map distances (in cM; Kosambi, 1944) are given on the right.

incongruity in the marker order between the two maps (in particular, the 28 cM interval between the markers Nv105 and Nv127 on chromosome 1; Figure 1). When we removed all markers with inconsistent positions of chromosome 1, the average difference in the recombination frequency of markers on this chromosome shrinked from 2.9% ($N=8$ genome segments) to 0.2% ($N=1$), and the genome-wide difference in recombination rate was 1.3% ($N=26$).

Embryonic versus adult F_2 hybrids: We were able to compare the recombination frequencies between embryos and adults of both reciprocal *N. vitripennis* × *N. giraulti* crosses for 34 genomic segments (Figure 3). Genome-wide differences in recombination frequencies of embryos and adults were small and not significant in either cross (absolute difference was 2.9% for the *N. giraulti* (♂) × *N. vitripennis* (♀) cross and 2.4% for the *N. vitripennis* (♂) × *N. giraulti* (♀) cross, $N=34$ genomic segments, Wilcoxon matched-pairs test, $P>0.05$; Figure 3).

The comparison of recombination frequencies between embryos and adults in the interspecific *N. vitripennis* × *N. longicornis* cross yielded comparable results (Figure 3). No significant genome-wide differences in recombination between embryos and adults were found in either cross (absolute difference between adults and embryos were 3.8% for hybrids with *N. vitripennis* cytoplasm and 3.9% for those with *N. longicornis* cytoplasm; $N=24$ genomic segments, Wilcoxon matched-pairs test, $P>0.05$). Recombination frequencies of adults versus adults and embryos versus embryos did not differ significantly between the reciprocal crosses of both species combinations either (Wilcoxon matched-pairs test, $P>0.05$).

Interspecific *N. vitripennis* × *N. giraulti* versus interspecific *N. vitripennis* × *N. longicornis* F_2 hybrids: Comparing F_2 hybrids with identical cytoplasm between interspecific *N. vitripennis* × *N. giraulti* and *N. vitripennis* × *N. longicornis* crosses did not indicate any significant differences in recombination rates for both adults and embryos ($N=12$ genomic segments; Wilcoxon matched-pairs test, $P>0.05$; Figure 4). The 12 marker intervals span a total of 199 cM, ~45% of the saturated high-density map (Niehuis *et al*., 2010). No matching intervals were available on chromosome 5, however. Hybrids

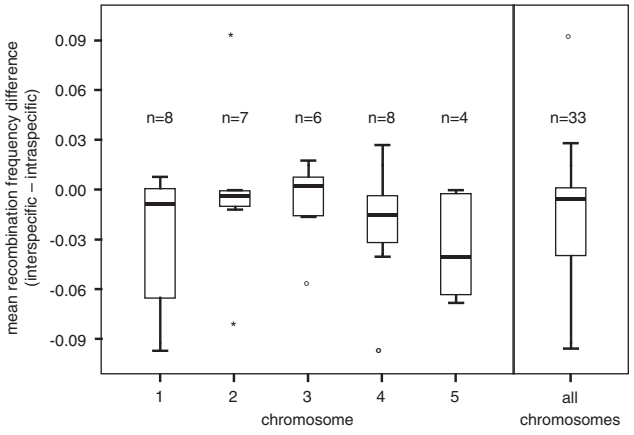

Figure 2 Comparison of recombination frequencies between *N. vitripennis* adult males and interspecific *N. giraulti* (♂) × *N. vitripennis* (♀) embryos. The left box plot shows differences in the recombination frequency between homologous genome segments per chromosome. The right plot depicts the differences pooled for the whole genome. In both cases, negative values indicate greater intraspecific recombination. Box plots show the median (thick horizontal line within the box), the 25 and 75 percentiles (box), and 1.5 times the interquartile range of the data (thin horizontal lines). Outliers are indicated by an open circle and extreme cases are marked by an asterisk.

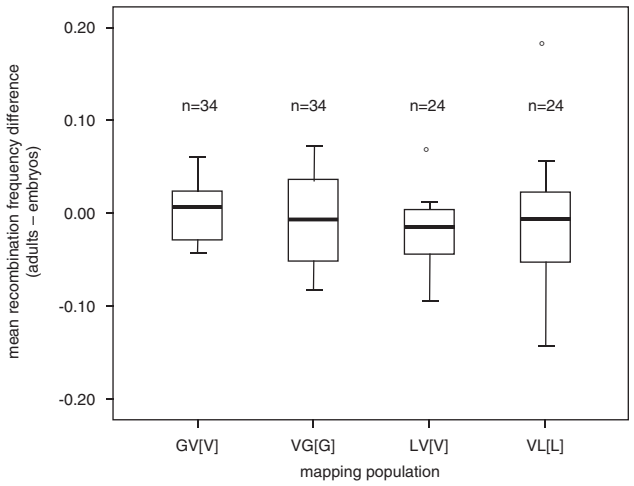

Figure 3 Comparison of recombination frequencies between mapping populations of F_2 hybrid embryos and adults from four interspecific crosses (*N. vitripennis* × *N. giraulti* and *N. vitripennis* × *N. longicornis* and the two respective reciprocal crosses). The nuclear genome of the parental species is indicated by a two-letter code (V = *N. vitripennis*, G = *N. giraulti*, L = *N. longicornis*). The genotype of the cytoplasm is shown in brackets (for example [V] = *N. vitripennis* cytoplasm). Negative values indicate greater recombination in embryos. Box plots show the median (thick horizontal line within the box), the 25 and 75 percentiles (box), and 1.5 times the interquartile range (thin horizontal lines) of the differences between homologous genome segments defined by flanking shared markers. Outliers are indicated by an open circle.

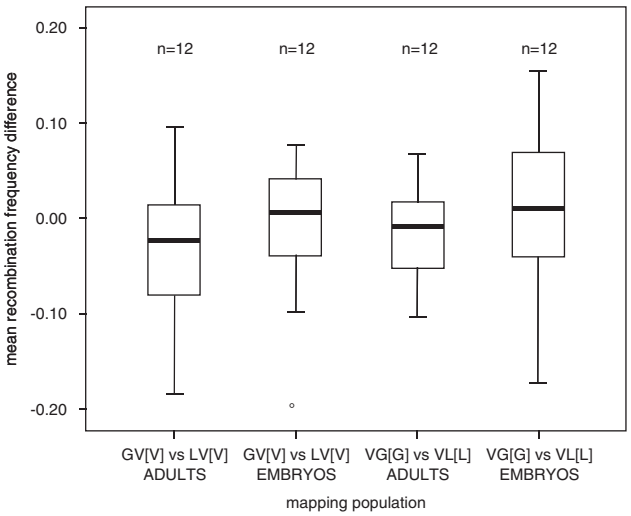

Figure 4 Comparison of the genome-wide recombination frequencies between eight independent interspecific mapping populations: adults and embryos of both reciprocal *N. vitripennis* × *N. giraulti* and *N. vitripennis* × *N. longicornis* crosses. The mean recombination frequency differences were not significantly different between the interspecific comparisons, irrespective of whether embryos or adults had been studied. The nuclear genome of the parental species is indicated by a two-letter code (V = *N. vitripennis*, G = *N. giraulti*, L = *N. longicornis*). Negative values indicate greater recombination in the mapping population given second in the comparison. The origin of the cytoplasm is shown in brackets (for example [V] = *N. vitripennis* cytoplasm). Box plots show the median (thick horizontal line within the box), the 25 and 75 percentiles (box), and 1.5 times the interquartile range (thin horizontal lines) of the data. Outliers are indicated by an open circle.

between *N. vitripennis* and *N. giraulti* and *N. longicornis*, respectively, did not show significant differences in recombination rates either ($N = 12$ genomic segments; Wilcoxon matched-pairs test, $P > 0.05$; Figure 4).

Discussion

The first genetic linkage map of *Nasonia* based on RAPD markers had been inferred by analyzing an interspecific cross between *N. vitripennis* and *N. giraulti* (Gadau *et al*., 1999). RAPD and AFLP markers typically show higher rates of deviation from expected Mendelian segregation ratios than microsatellite markers (Voorrips *et al*., 1997; Tan *et al*., 2001; Zhang *et al*., 2007), likely because of genotyping errors. We found the same to be true for *Nasonia* (RAPD: C Pietsch, unpublished; AFLP: LW Beukeboom, unpublished). The first microsatellite markers for *Nasonia* were developed by Pietsch *et al*. (2004) and Rütten *et al*. (2004). The recently published genome sequences of three *Nasonia* species made it possible to rapidly develop additional microsatellite markers with both intraspecific variability and species–specific alleles (Pannebakker *et al*., 2010). These newly developed markers allowed us to quickly construct the first intraspecific linkage map for *N. vitripennis* based on molecular markers and to infer additional interspecific maps as well (that is *N. vitripennis* × *N. longicornis*).

One potential problem with genotyping interspecific hybrids for genome mapping are deleterious interactions between the two genomes that can result in MTRD, in particular, in haploid males in which recessive deleterious interactions are not masked. Crosses between *Nasonia* species are known to result in nucleo–nucleo and nucleo–cytoplasmic (= cytonuclear) genic incompatibilities that cause an increase in hybrid mortality during larval development (Breeuwer and Werren, 1995; Gadau *et al*., 1999; Niehuis *et al*., 2008). A major concern in *Nasonia* research on speciation and species differences when studying interspecific hybrids has therefore been whether interspecific linkage maps accurately reflect the order and distance between markers. This concern led Niehuis *et al*. (2008) to compare allele recovery rates between embryos and adults of interspecific hybrids. On four of the five chromosomes, they found at least one region at which markers were significantly distorted. Using the same samples as these authors, we found, however, that the presence of such distorters do not significantly affect the observed genome-wide recombination frequencies, as the linkage maps based on embryos or adults have similar sizes (Figure 2). Since we compared recombination frequencies between adjacent markers that were shared between two mapping populations, our results are not obscured by differences in the size of the maps or their coverage of the genome. We found that intraspecific recombination rates were only slightly higher (1.8%) than interspecific rates, which indicates that the observed genic incompatibilities between *Nasonia* species do not severely increase or decrease recombination

We found one major incongruence in the marker order between the intraspecific *N. vitripennis* and the interspecific *N. vitripennis* × *N. giraulti* map. Although we cannot rule out a genomic inversion in one of the two species, we think that this finding likely reflects a mapping error because we do not find such a difference

in the marker order in any of the other crosses. Thus, when comparing the recombination frequencies between different interspecific crosses with either the same or with a different cytoplasm (Figure 4), we found no significant difference. We had not been able to include markers on chromosome 5 in the interspecific map comparisons. However, our comparison of the intraspecific *N. vitripennis* map with the interspecific *N. vitripennis* × *N. giraulti* map did include four marker intervals on this chromosome. Chromosome 5, together with chromosome 1, showed the largest deviation in recombination frequencies between mapping populations. As mapping populations of embryonic and adult F_2 hybrids did not differ significantly in their recombination frequencies, we conclude that interspecific crosses with adult individuals do not greatly impair mapping studies in *Nasonia*. However, we nonetheless advice caution when interpreting differences in recombination frequencies on chromosomes 1 and 5 between mapping populations.

Future studies that address the comparative genomics of closely related species will provide important additional data on the speed and mode of genome evolution, and the *Nasonia* clade may well have an important function (Werren *et al*., 2010). With such information at hand, we may gain further insights of the extent to which phylogenetic distance maps to major genomic differences and of the forces that drive the evolution of genomic changes (Lynch, 2007). Comparison of recombination frequencies and the degree of synteny between related species allows us to infer the function of chromosomal rearrangements in species divergence (Ortiz-Barrientos *et al*., 2002). Recombination frequencies in interspecific hybrids have been well studied in plants in the context of polyploidization and selective breeding of cultured plant species. These studies revealed major alterations of meiotic pairing leading to distortions in recombination frequencies (Zhang *et al*., 1999). For example, Llopart *et al*. (2005) found that the degree of introgression between *Drosophila yakuba* and *D. santomea* depends on the region in the genome and the associated recombination rate. Recombination between divergent genomes in hybrids may be selectively disadvantageous, because it often leads to hybrid dysgenesis, with a proportionally large effect of the sex chromosomes (Coyne and Orr, 2004). However, beneficial effects have been reported too (for example Edmands, 2008). *Nasonia* wasps are haplodiploid and do not have sex chromosomes, yet interspecific crosses do result in increased mortality of F_2 hybrid males (Breeuwer and Werren, 1995; Gadau *et al*., 1999; Bordenstein and Werren, 1999; Niehuis *et al*., 2008; Koevoets and Beukeboom, 2009; Koevoets, unpublished). We found no evidence for major genome rearrangements between the three *Nasonia* species. However, our genome coverage was only 70% (intraspecific *N. vitripennis* versus interspecific *N. vitripennis* × *N. giraulti* map) and 45% (interspecific *N. vitripennis* × *N. giraulti* versus *N. vitripennis* × *N. longicornis* map), respectively, and chromosome 5 was not included in the latter comparison. Interestingly, both Niehuis *et al*. (2008) and Koevoets (unpublished) have identified chromosome 5 as being involved in male F_2 hybrid male breakdown. Hence, it remains to be seen to what extent hybrid breakdown in *Nasonia* is due to detrimental epistatic interactions between genes or due to chromosomal rearrangements.

Conflict of interest

The authors declare no conflict of interest.

Acknowledgements

LWB, BAP, and TK acknowledge the Netherlands Organization for Scientific Research NWO/ALW (grants 863.08.008, 816.01.004, and 833.02.003). ON acknowledges the Alexander von Humboldt Foundation for a Feodor Lynen Research Fellowship for Postdoctoral Researchers. BAP and DMS were supported by the National Environment Research Council. JG was supported by a grant from the National Institutes of Health (NIH 1R21 RR024199-01). We are indebted to two anonymous reviewers for valuable comments on an earlier version of the paper.

References

Bordenstein SR, Werren JH (1999). Effects of A and B *Wolbachia* and host genotype on interspecies cytoplasmic incompatibility between two *Nasonia* species. *Genetics* **148**: 1833–1844.

Breeuwer JAJ, Werren JH (1995). Hybrid breakdown between two haplodiploid species: the role of nuclear and cytoplasmic genes. *Evolution* **49**: 705–717.

Burton-Chellew MN, Koevoets T, Grillenberger BK, Sykes EM, Underwood SL, Bijlsma K *et al*. (2008). Facultative sex ratio adjustment in natural populations of wasps: cues of local mate competition and the precision of adaptation. *Am Nat* **172**: 393–404.

Campbell BC, Steffen-Campbell JD, Werren JH (1993). Phylogeny of the *Nasonia* species complex (Hymenoptera: Pteromalidae) inferred from an rDNA internal transcribed spacer (ITS2). *Insect Mol Biol* **2**: 225–237.

Chen D, Berger J, Fellner M, Suzuki T (2009). FLYSNPdb: a high-density SNP database of *Drosophila melanogaster*. *Nucleic Acids Res* **37**: D567–D570.

Coyne J, Orr A (2004). *Speciation*. Sinnauer Associates: Sunderland, MA.

Darling DC, Werren JH (1990). Biosystematics of *Nasonia* (Hymenoptera: Pteromalidae): two new species reared from birds' nests in North America. *Ann Entomol Soc Am* **83**: 352–370.

Edmands S (2008). Recombination in interpopulation hybrids of the copepod *Tigriopus californicus*: release of beneficial variation despite hybrid breakdown. *J Hered* **99**: 316–318.

Fulton RE, Salasek ML, Duteau MN, Black WC (2001). SSC analysis of cDNA markers provides a dense linkage map of the *Aedes aegypti* genome. *Genetics* **158**: 715–726.

Gadau J, Page RE, Werren JH (1999). Mapping hybrid incompatibility loci in *Nasonia*. *Genetics* **153**: 1731–1741.

Gadau J, Niehuis O, Peire A, Werren JH, Baudry E, Beukeboom LW (2008). The jewel wasp—*Nasonia*. In: Hunter W, Kole C (eds). *Genome Mapping and Genomics in Animals*. Springer Verlag: Berlin Heidelberg. pp 27–41.

Gokhman VE, Westendorf M (2000). The chromosomes of three species of the *Nasonia* complex (Hymenoptera, Pteromalidae). *Beitr Entomol Suppl* **50**: 193–198.

Hunter W, Kole C (2008). *Genome Mapping and Genomics in Animals*. Springer Verlag: Berlin Heidelberg.

Koevoets T, Beukeboom LW (2009). Genetics of postzygotic isolation and Haldane's rule in haplodiploids. *Heredity* **102**: 16–23.

Kosambi DD (1944). The estimation of map distances from recombination values. *Ann Eugen* **12**: 172–175.

Kulathinal RJ, Bennett SM, Fitzpatrick CL, Noor MAF (2008). Fine-scale mapping of recombination rate in *Drosophila*

refines its correlation to diversity and divergence. *Proc Natl Acad Sci USA* **105**: 10051–10056.

Llopart A, Lachaise D, Coyne JA (2005). Multilocus analysis of introgression between two sympatric sister species of *Drosophila*: *Drosophila yakuba* and *D santomea*. *Genetics* **171**: 197–210.

Lorenzen MD, Doyungan Z, Savard J, Snow K, Crumly LR, Shippy TD *et al.* (2005). Genetic linkage maps of the red flour beetle, *Tribolium castaneum*, based on bacterial artificial chromosomes and expressed sequence tags. *Genetics* **170**: 741–747.

Lynch M (2007). The frailty of adaptive hypotheses for the origins of organismal complexity. *Proc Nat Acad Sci USA* **104**: 8597–8604.

Mester DI, Ronin YI, Hu Y, Peng J, Nevo E, Korol AB (2003a). Efficient multipoint mapping: making use of dominant repulsion-phase markers. *Theor Appl Genet* **107**: 1102–1112.

Mester DI, Ronin YI, Minkov D, Nevo E, Korol AB (2003b). Constructing large-scale genetic maps using an evolutionary strategy algorithm. *Genetics* **165**: 2269–2282.

Mester DI, Ronin YI, Nevo E, Korol AB (2004). Fast and high precision algorithms for optimization in large-scale genomic problems. *Comput Biol Chem* **28**: 281–290.

Myers S, Bottolo L, Frreeman C, McVean G, Donnelly P (2005). A fine-scale map of recombination rates and hotspots across the human genome. *Science* **310**: 321–324.

Niehuis O, Judson AK, Gadau J (2008). Cytonuclear genic incompatibilities cause increased mortality in male F_2 hybrids of *Nasonia giraulti* and *N vitripennis*. *Genetics* **178**: 413–426.

Niehuis O, Gibson JD, Rosenberg MS, Pannebakker BA, Koevoets T, Judson AK *et al.* (2010). Recombination and its impact on the genome of the haplodiploid parasitoid wasp *Nasonia*. *PLoS ONE* (doi:10.1371/journal.pone.0008597).

Ortiz-Barrientos D, Reiland J, Hey J, Noor MAF (2002). Recombination and the divergence of hybridizing species. *Genetica* **116**: 167–178.

Pannebakker BA, Halligan DL, Reynolds KT, Ballantyne GA, Shuker DM, Barton NH *et al.* (2008). Effects of spontaneous mutation accumulation on sex ratio traits in a parasitoid wasp. *Evolution* **62**: 1921–1935.

Pannebakker BA, Niehuis O, Hedley A, Gadau J, Shuker DM (2010). The distribution and evolution of microsatellites in the *Nasonia* parasitoid wasp genome. *Insect Mol Biol* **19**: 91–98.

Petes TD (2001). Meiotic recombination hot spots and cold spots. *Nat Rev Genet* **2**: 360–369.

Pietsch C, Rütten K, Gadau J (2004). Eleven microsatellite markers in *Nasonia*, Ashmead 1904 (Hymenoptera; Pteromalidae). *Mol Ecol Notes* **4**: 43–45.

Raychoudhury R, Desjardins CA, Buellesbach J, Loehlin DW, Grillenberger BK, Beukeboom LW *et al.* (2010). Behavioural and genetic characteristics of a new species of *Nasonia*. *Heredity* (doi:10.1038/hdy.2009.147).

Rütten KB, Pietsch C, Olek K, Neusser M, Beukeboom LW, Gadau J (2004). Chromosomal anchoring of linkage groups and identification of wing size QTL using markers and FISH probes derived from microdissected chromosomes in *Nasonia* (Pteromalidae: Hymenoptera). *Cytogenet Genome Res* **105**: 126–133.

Saul GB, Kayhart M (1956). Mutants and linkage in *Mormoniella*. *Genetics* **41**: 930–937.

Saul GB (1993). Gene map of the parasitic wasps *Nasonia vitripennis* (=*Mormoniella vitripennis*) (2N = 10). In: O'Brien SJ (ed). *Genetic Maps. Locus Maps of Complex Genomes*. Cold Spring Harbor Laboratory Press: Cold Spring Harbor, NY. pp **3**: 193–198. .201.

Solignac M, Mougel F, Vautrin D, Monnerot M, Cornuet J-M (2007). A third-generation microsatellite-based linkage map of the honeybee, *Apis mellifera*, and its comparison with the sequence-based physical map. *Genome Biol* **8**: R66.

Tan YD, Wan C, Zhu Y, Lu C, Xiang Z, Deng HW (2001). An amplified fragment length polymorphism map of the silkworm. *Genetics* **157**: 1277–1284.

Trickett AJ, Butlin RK (1994). Recombination suppressors and the evolution of new species. *Heredity* **73**: 339–345.

Voorrips RE, Jogerius MC, Kanne HJ (1997). Mapping of two genes for resistance to clubroot (*Plasmodiphora brassicas*) in a population of doubled haploid lines of *Brassica oleracea* by means of RFLP and AFLP markers. *Theor Appl Genet* **94**: 75–82.

Werren JH, Richards S, Desjardins CA, Niehuis O, Gadau J, Colbourne JK *et al.* (2010). Functional and evolutionary insights from the genomes of three parasitoid *Nasonia* species. *Science* **327**: 343.

Weston RF, Qureshi I, Werren JH (1999). Genetics of wing size difference between two *Nasonia* species. *J Evol Biol* **12**: 586–595.

Whiting AR (1967). The biology of the parasitic wasp *Mormoniella vitripennis* [=*Nasonia brevicornis*] (Walker). *Q Rev Biol* **42**: 333–406.

Wilfert L, Gadau J, Schmid-Hempel P (2007). Variation in genomic recombination rates among animal taxa and the case of social insects. *Heredity* **98**: 189–197.

Yamamoto K, Narukawa J, Kadono-Okuda K, Nohata J, Sasanuma M, Suetsugu Y *et al.* (2006). Construction of a single nucleotide polymorphism linkage map for the silkworm, *Bombyx mori*, based on artificial chromosome end sequences. *Genetics* **173**: 151–161.

Zhang L, Pickering R, Murray B (1999). Direct measurement of recombination frequency in interspecific hybrids between *Hordeum vulgare* and *H* bulbosum using genomic in-situ hybridization. *Heredity* **83**: 304–309.

Zhang L, Yang C, Zhang Y, Li L, Zhang X, Zhang Q *et al.* (2007). A genetic linkage map of Pacific white shrimp (*Litopenaeus vannamei*): sex linked microsatellite markers and high recombination rates. *Genetica* **31**: 37–49.

Supplementary Information accompanies the paper on Heredity website (http://www.nature.com/hdy)